

This copy is for your personal, non-commercial use only.

If you wish to distribute this article to others, you can order high-quality copies for your colleagues, clients, or customers by [clicking here](#).

Permission to republish or repurpose articles or portions of articles can be obtained by following the guidelines [here](#).

The following resources related to this article are available online at www.sciencemag.org (this information is current as of April 23, 2014):

Updated information and services, including high-resolution figures, can be found in the online version of this article at:

<http://www.sciencemag.org/content/333/6050/1764.full.html>

Supporting Online Material can be found at:

<http://www.sciencemag.org/content/suppl/2011/09/22/333.6050.1764.DC1.html>

A list of selected additional articles on the Science Web sites **related to this article** can be found at:

<http://www.sciencemag.org/content/333/6050/1764.full.html#related>

This article **cites 21 articles**, 10 of which can be accessed free:

<http://www.sciencemag.org/content/333/6050/1764.full.html#ref-list-1>

This article has been **cited by** 9 articles hosted by HighWire Press; see:

<http://www.sciencemag.org/content/333/6050/1764.full.html#related-urls>

This article appears in the following **subject collections**:

Microbiology

<http://www.sciencemag.org/cgi/collection/microbio>

binding of solubilized ZP to capacitated spermatozoa (Fig. 4E).

Previous studies indicated that antibodies directed against sialyl-Lewis^a, sialyl-Lewis^x, and Lewis^b epitopes react with human ZP (22, 23). The antibody to Lewis^b blocked human sperm-ZP binding in the hemizona assay (22). Erythroagglutinating phytohemagglutinin also binds to human ZP, indicating that bisecting type N-glycans are expressed on this matrix (24). However, the current results have established that only the sialyl-Lewis^x antigen is expressed at physicochemically confirmable levels on ZP. Based on assessments of signal-to-noise ratio for detected molecular and fragment ions, it was estimated that other antigens must be substantially less than 1% of the glycome. The biophysical analyses here confirm the expression of carbohydrate sequences. Antibodies and lectins are useful for detecting carbohydrate ligands once their existence is confirmed, but they would not detect the multivalent presentations of sialyl-Lewis^x and sialyl-Lewis^x-Lewis^x sequences.

Little is known about how human spermatozoa bind to eggs. The work described here provides insight into the key binding interactions that are essential for natural human fertilization, supporting the hypothesis that human gamete binding primarily involves the participation of

the selectin ligand sialyl-Lewis^x. Because human spermatozoa do not express selectins (25), the major egg-binding protein is very likely a lectin with a binding specificity that overlaps with the selectins.

References and Notes

- K. J. Mengerink, V. D. Vacquier, *Glycobiology* **11**, 37R (2001).
- P. M. Wassarman, L. Jovine, E. S. Litscher, *Nat. Cell Biol.* **3**, E59 (2001).
- T. T. F. Huang, E. Ohzu, R. Yanagimachi, *Gamete Res.* **5**, 355 (1982).
- L. M. Stoolman, S. D. Rosen, *J. Cell Biol.* **96**, 722 (1983).
- L. A. Lasky, *Science* **258**, 964 (1992).
- M. Fukuda, N. Hiraoka, J. C. Yeh, *J. Cell Biol.* **147**, 467 (1999).
- M. S. Patankar, S. Oehninger, T. Barnett, R. L. Williams, G. F. Clark, *J. Biol. Chem.* **268**, 21770 (1993).
- S. J. North *et al.*, *Methods Enzymol.* **478**, 27 (2010).
- P. C. Pang *et al.*, *J. Biol. Chem.* **282**, 36593 (2007).
- A. Varki *et al.*, Eds., *Essentials of Glycobiology* (Cold Spring Harbor Laboratory Press, Cold Spring Harbor, NY, 2009).
- P. Babu *et al.*, *Glycoconj. J.* **26**, 975 (2009).
- F. J. Schweigert, B. Gericke, W. Wolfram, U. Kaisers, J. W. Dudenhausen, *Hum. Reprod.* **21**, 2960 (2006).
- M. Ferens-Sieczkowska, M. Olczak, *Z. Naturforsch. C* **56**, 122 (2001).
- Y. Mechref *et al.*, *J. Proteome Res.* **8**, 2656 (2009).
- Y. Imai, L. A. Lasky, S. D. Rosen, *Nature* **361**, 555 (1993).
- S. D. Rosen, *Annu. Rev. Immunol.* **22**, 129 (2004).
- K. H. Khoo, S. Y. Yu, *Methods Enzymol.* **478**, 3 (2010).
- J. L. Magnani, *Glycobiology* **1**, 318 (1991).

- E. C. Brinkman-van der Linden, E. C. van Ommen, W. van Dijk, *Glycoconj. J.* **13**, 27 (1996).
- M. Fukuda *et al.*, *J. Biol. Chem.* **260**, 12957 (1985).
- P. C. Chiu *et al.*, *Biol. Reprod.* **79**, 869 (2008).
- H. Lucas *et al.*, *Hum. Reprod.* **9**, 1532 (1994).
- M. Jiménez-Movilla *et al.*, *Hum. Reprod.* **19**, 1842 (2004).
- M. S. Patankar *et al.*, *Mol. Hum. Reprod.* **3**, 501 (1997).
- G. F. Clark, M. S. Patankar, K. D. Hinsch, S. Oehninger, *Hum. Reprod.* **10** (suppl. 1), 31 (1995).

Acknowledgments: This work was supported by the Biotechnology and Biological Sciences Research Council (BBSRC), grant BBF0083091 (to A.D., H.R.M., and S.M.H.); a Royal Society International Joint Project Award (to A.D. and K-H.K.); the Breedon-Adams Foundation and a Life Sciences Mission Enhancement Reproductive Biology Program funded by the state of Missouri (to G.F.C.); and the University Research Committee, University of Hong Kong (to P.C.N. and W.S.B.Y.). The proteomics and sulfoglycomics data were acquired at the National Research Program for Genomic Medicine (NRPGM) Core Facilities for Proteomics and Glycomics funded by the Taiwan National Science Council (NSC99-3112-B-001-025). An intellectual property disclosure has been filed with the University of Missouri that covers technology described in this paper.

Supporting Online Material

www.sciencemag.org/cgi/content/full/science.1207438/DC1

Materials and Methods

Figs. S1 to S10

Table S1

References (26–35)

25 April 2011; accepted 10 August 2011

Published online 18 August 2011;

10.1126/science.1207438

Acceleration of Emergence of Bacterial Antibiotic Resistance in Connected Microenvironments

Qiucen Zhang,¹ Guillaume Lambert,¹ David Liao,² Hyunsung Kim,³ Kristelle Robin,⁴ Chih-kuan Tung,⁵ Nader Pourmand,³ Robert H. Austin^{1,4*}

The emergence of bacterial antibiotic resistance is a growing problem, yet the variables that influence the rate of emergence of resistance are not well understood. In a microfluidic device designed to mimic naturally occurring bacterial niches, resistance of *Escherichia coli* to the antibiotic ciprofloxacin developed within 10 hours. Resistance emerged with as few as 100 bacteria in the initial inoculation. Whole-genome sequencing of the resistant organisms revealed that four functional single-nucleotide polymorphisms attained fixation. Knowledge about the rapid emergence of antibiotic resistance in the heterogeneous conditions within the mammalian body may be helpful in understanding the emergence of drug resistance during cancer chemotherapy.

The systematic emergence of antibiotic resistance in bacteria remains a persistent problem worldwide (1). Genetic analyses

following the isolation of resistant mutants have shed light on the biological processes that are altered in mutant bacteria (2–4); however, such studies fail to probe how such mutations occur and spread within a population during antibiotic treatment. In particular, the importance of spatial heterogeneities and their effect on evolutionary processes during the emergence of antibiotic resistance is often overlooked. Sewall Wright understood that the dynamics of evolution of individuals on a heterogeneous fitness landscape could be accelerated if the population were broken up into smaller populations with weak inter-

change of mutant individuals among the populations (5, 6). A spatially complex environment may lead to an enhanced rate of evolution for two reasons. First, if a stress gradient is imposed on a connected network of populations, and if a mutant acquires some resistance to the local stress, the relative fitness of the mutant is increased if it moves to join a population exposed to even higher stress. Second, because there are fewer individuals in the region of higher stress, the mutant can fix more quickly in the smaller population.

Recent modeling efforts (7) have predicted that in a heterogeneous environment, accelerated evolution should occur. Testing of emergence dynamics requires the construction of a simplified network of ecological niches that can be observed continuously and can capture the complexity of the external world. Microfabrication technology is well suited for constructing arrays in which ranges of physicochemical conditions can be established that resemble heterogeneous ecological niches. The device we designed was intended to capture many of the features that give rise to rapid emergence of resistance in more complex environments, such as those occurring within soil or host animals.

Our device consisted of 1200 hexagonal wells etched 10 μm deep into a silicon wafer. Each well had sides 200 μm long and was connected to its nearest neighbors via six microchannels that were 200 μm long, 10 μm deep, and 10 μm wide (fig. S1). Nanoslits 100 nm deep were etched into the sidewalls of the peripheral wells at the edge of the array to allow nutrients and antibiotic to flow into the interior of the array. We used ciprofloxacin,

¹Department of Physics, Princeton University, Princeton, NJ 08544, USA. ²Department of Pathology, University of California, San Francisco, CA 94143, USA. ³University of California, Santa Cruz Genome Sequencing Center, University of California, Santa Cruz, CA 95064, USA. ⁴Institute for Advanced Study, Hong Kong University of Science and Technology, Kowloon, Hong Kong. ⁵Department of Physics, University of Pittsburgh, Pittsburgh, PA 15260, USA.

*To whom correspondence should be addressed. E-mail: austin@princeton.edu

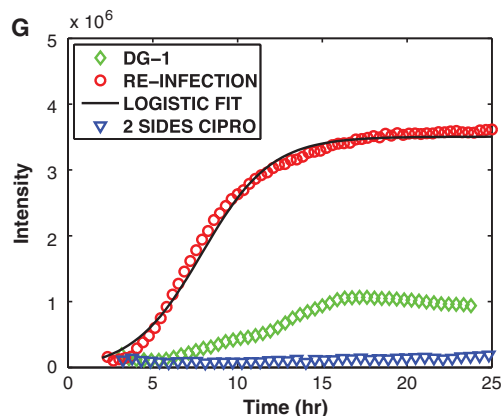
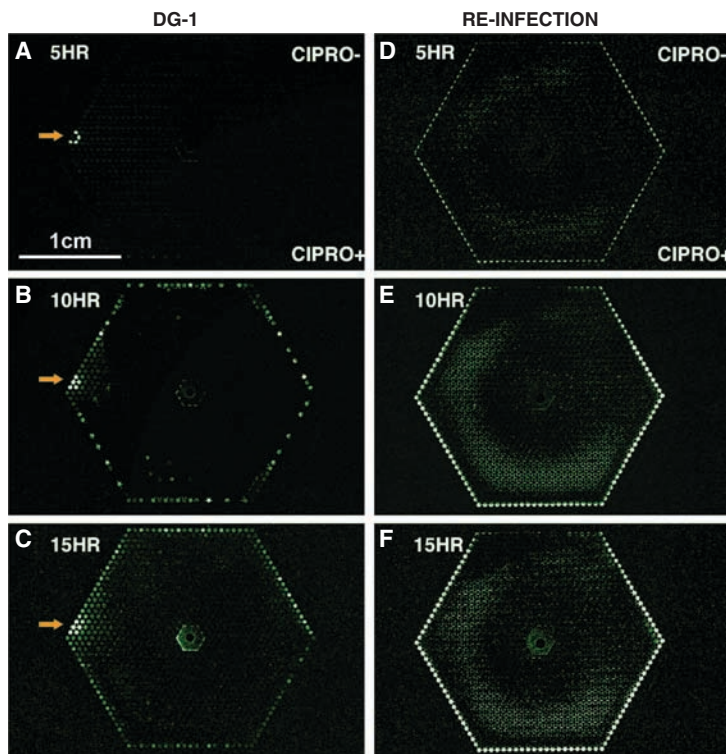


Fig. 1. (A to C) Initial inoculations of 10^6 wild-type bacteria with ciprofloxacin ($10 \mu\text{g/ml}$) in the bottom channel. (A) Emergence of resistance to ciprofloxacin ~ 5 hours after inoculation. The Goldilocks microenvironment is shown by the orange arrow. (B) Spread of resistant bacteria around the periphery of the microenvironments at 10 hours after inoculation. (C) Continued growth of ciprofloxacin-resistant bacteria after 15 hours. (D to F) Growth of resistant mutant bacteria upon re-inoculation in a new chip with the same culture conditions as in (A) to (C). (G) Summed growth over the entire chip versus time, shown for wild-type bacteria (green diamonds), re-inoculated mutants (red circles), and wild-type bacteria with ciprofloxacin flowing on both sides (blue triangles). A logistic fit is shown for the growth of re-inoculated mutant bacteria (black line).

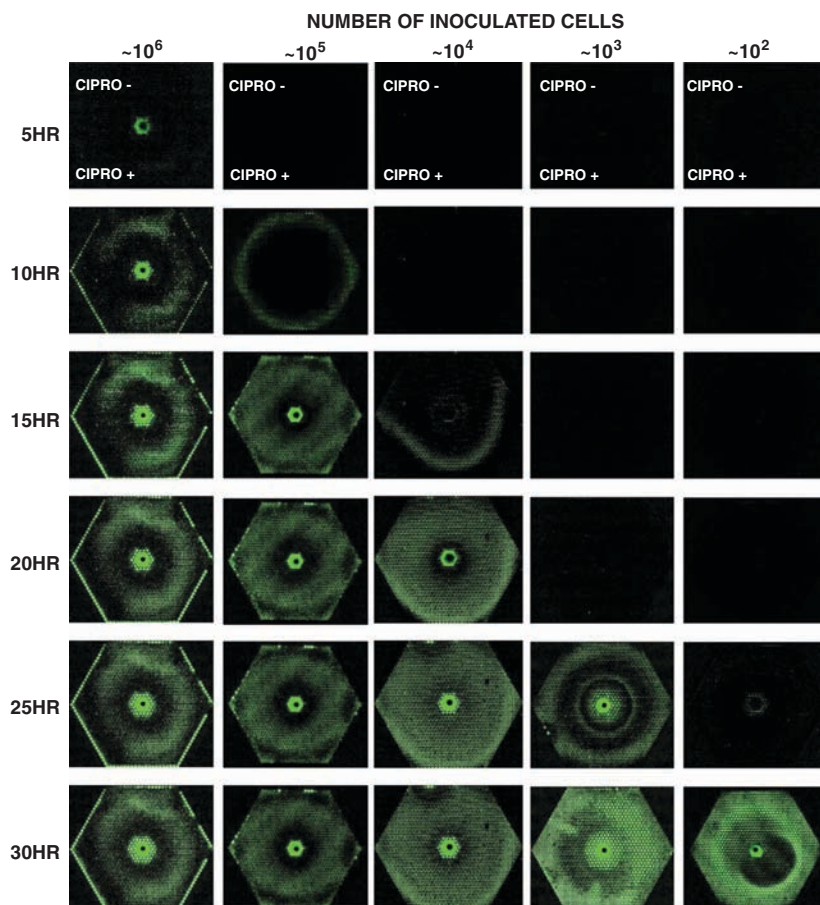


Fig. 2. Bacterial density versus time, shown for initial inoculations of 10^6 , 10^5 , 10^4 , 10^3 , and 10^2 wild-type *E. coli* with ciprofloxacin ($1 \mu\text{g/ml}$) in the bottom channel.

a clinically relevant genotoxic antibiotic (8) and a member of the quinolone family of antibiotics (9), as the stressor across the array. Ciprofloxacin traps the gyrase-DNA complex, inhibiting DNA replication and cell division but not killing the cell (10–14). Two separate syringe pumps created the stressor gradient: One pump circulated Luria-Bertani (LB) broth around the top of the array, and the other pump circulated LB broth containing ciprofloxacin ($10 \mu\text{g/ml}$) around the bottom of the array. A stable gradient of antibiotic was established across the array by pumping counter-moving flows of LB broth and LB broth + ciprofloxacin around the periphery for 24 hours at a rate of $30 \mu\text{l/hour}$ in each arm. Bacteria were inoculated into the center of the array via a hole drilled through the center of the device. For each experiment, $2 \mu\text{l}$ of bacteria culture were introduced into the device before sealing the hole with silicone elastomer. A 470-nm LED (Thorlabs) and a Canon 5D charge-coupled device camera were used to obtain images of green fluorescent protein (GFP)-labeled bacteria for 48 hours after inoculation.

Rapid emergence of ciprofloxacin resistance occurred in wild-type *E. coli* with an inoculation number of 10^6 wild-type bacteria and an external ciprofloxacin concentration of $10 \mu\text{g/ml}$ maintained in the bottom channel (Fig. 1). This concentration, $10 \mu\text{g/ml}$, is about 200 times the minimum inhibitory concentration (MIC) of ciprofloxacin (14, 15). When bacteria were inoculated into the center of the device, chemotaxis driven by consumption of nutrients quickly concentrated bacteria at the perimeter of the

device against the nanoslits (16, 17). Microenvironments on the chip, which we call “Goldilocks points,” correspond to regions where the local density of bacteria is a strong function of the antibiotic gradient. We observed that motile mutants moved rapidly to regions of increased antibiotic concentration, where they fixed rapidly. Once resistant mutants fixed at a Goldilocks local microenvironment, a propagating front of resistant bacteria invaded the entire chip (movie S1). The Goldilocks phenomenon was initially revealed by bursts of bacterial growth at the convergence of the ciprofloxacin-containing and

antibiotic-free broth flows, where the stress gradients were highest. The mixture of wild-type and mutant bacteria competing for resources led to complex integrated growth dynamics (Fig. 1G). Extraction of the resistant *E. coli* by replica plating and reintroduction into a new chip (15) showed that the resistant bacteria grew exponentially, with higher fitness prevailing on the LB + ciprofloxacin side of the device (Fig. 1F).

We used two methods to verify the importance of the antibiotic gradients for the development of resistance across the array: (i) eliminating the antibiotic gradients in the chip itself by flowing

ciprofloxacin around both sides of the device, and (ii) recreating our antibiotic and nutrient landscape in a 96-well format consisting of discrete wells. No growth of the wild-type bacteria occurred when ciprofloxacin was applied uniformly across the chip (Fig. 1G) (15). Two separate arrays were inoculated with either wild-type bacteria or resistant bacteria sampled from the chip. The 96-well array inoculated with wild-type bacteria showed rapid loss of fitness with increasing ciprofloxacin, no growth at high ciprofloxacin concentrations, and a fitness landscape with a single peak at the lowest ciprofloxacin and highest nutrient concentrations (fig. S2). The role of motility in the rapid emergence of resistance was tested using LB agar plates with a ciprofloxacin gradient over the same range of concentrations as in the chip. However, when 10^8 wild-type *E. coli* were spread over this plate, the bacteria showed no motility; bacterial colonies grew below the MIC, with no emergence of resistance (fig. S3).

We next investigated whether the resistant bacteria that emerged were the progeny of pre-existing mutant bacteria, or whether they evolved in response to the antibiotic stress in the ecological niches. If preexisting mutants were the origin of resistance, then growth would have occurred above the MIC in the 96-well experiment (15) (fig. S2). This did not happen. If resistance was due to pre-existing but rare mutants, then upon serial dilution and inoculation, we should reach an initial inoculation density where no preexisting resistant

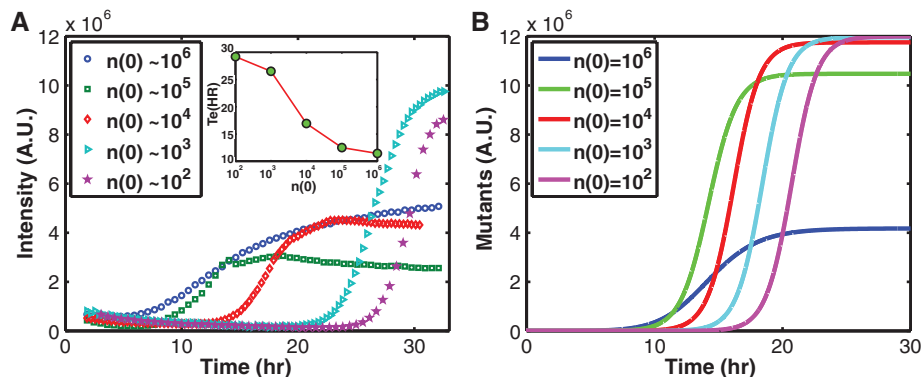


Fig. 3. (A) Integrated intensity [in arbitrary units (A.U.)] versus time for initial inoculations of 10^6 , 10^5 , 10^4 , 10^3 , and 10^2 bacteria. Inset shows the scaling of emergent time T_e versus the number of wild-type cells inoculated into the device. (B) Mean-field simulation of the model of the emergence of resistance as a function of initial inoculation numbers.

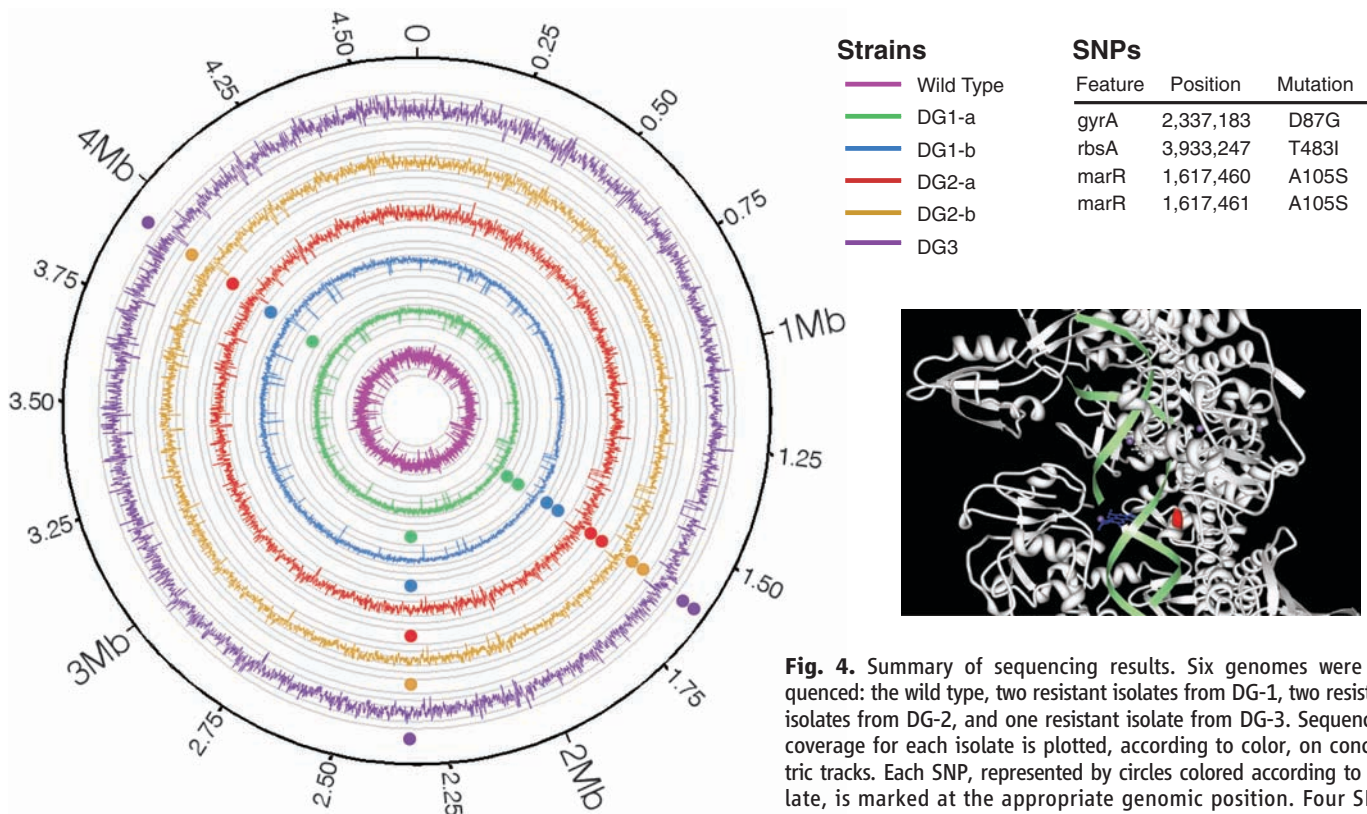


Fig. 4. Summary of sequencing results. Six genomes were sequenced: the wild type, two resistant isolates from DG-1, two resistant isolates from DG-2, and one resistant isolate from DG-3. Sequencing coverage for each isolate is plotted, according to color, on concentric tracks. Each SNP, represented by circles colored according to isolate, is marked at the appropriate genomic position. Four SNPs were found in five strains sampled from three independent experiments with initial inoculation of 10^6 *E. coli*. Lower right: X-ray structure of *gyrA* + double-stranded DNA (green helix), ciprofloxacin (blue), and the local SNP site (red) in *gyrA*.

bacterium exists. We conducted five experiments with initial inoculation numbers of 10^6 , 10^5 , 10^4 , 10^3 , and 10^2 wild-type *E. coli*. A mosaic of resistant bacteria emerged at all the different inoculation levels (Fig. 2), and even at inoculations of as few as 100 bacteria, resistance emerged; these results support the occurrence of de novo mutation. We developed a simple model (15) that predicted that as the initial number of wild-type bacteria inoculated (n_0) is decreased, the time for the emergence of de novo resistance increases but remains finite. A comparison of the data with the mean-field simulation of the model shows approximate agreement with the data (Fig. 3).

We examined whole genome sequences to understand what mutations occurred and spread within the population. Baseline sequences were obtained from the wild-type bacteria before introduction to the chip, and single-nucleotide polymorphisms (SNPs) were counted only if they did not appear in the wild-type base sequences. The experiment with 10^6 wild-type *E. coli* inoculations was repeated three times and whole genome sequences were obtained independently for each.

Four SNPs were found in each of the three experiments (DG-1, DG-2, DG-3) (Fig. 4). The four SNPs that fix are clearly functional SNPs that give rise to resistance: First, a T → C mutation in base 2,337,183 of the *E. coli* K12 genome causes an Asp⁸⁷ → Gly missense mutation in *gyrA*. Structural alignment of the protein sequences of the *E. coli* and *Staphylococcus aureus* gyrase A subunits revealed that *E. coli* Asp⁸⁷ aligned to *S. aureus* Glu⁸⁸. Asp and Glu differ by a single carbon, and these two residues are often substituted in similar proteins. Reconstructing this mutation in the known x-ray structure of *S. aureus* gyrase A (18) reveals that ciprofloxacin inhibits *gyrA* function by sitting in the active site of the enzyme, and the mutated amino acid (red in

Fig. 4) sits very close to ciprofloxacin. Thus, this SNP is likely to be functional.

Second, a missense A → T in base 3,933,247 in a region coding for the *rbsA* gene, which is a component of the ribose ABC transporter complex, has been previously reported to export other antibiotics (erythromycin, tylosin, and macrolides) (19). Thus, this SNP is also likely to be functional.

The third and fourth mutations constituted a pair of missense SNPs (C → G in base 1,617,460; A → C in base 1,617,461) in the coding sequence for *marR*. The normal function of *marR* is to repress the multiple antibiotic resistance (*mar*) operon (20). It is possible that these SNPs alter the ability of *E. coli* to regulate the expression of antibiotic resistance genes.

It is surprising that four apparently functional SNPs should fix in a population within 10 hours of exposure to antibiotic in our experiment. A detailed understanding of the order in which the SNPs occur is essential, but it is unlikely that the four SNPs emerged simultaneously; in all likelihood they are sequential (21–23). The device and data we have described here offer a template for exploring the rates at which antibiotic resistance arises in the complex fitness landscapes that prevail in the mammalian body. Furthermore, our study provides a framework for exploring rapid evolution in other contexts such as cancer (24).

References and Notes

1. S. B. Levy, B. Marshall, *Nat. Med.* **10**, 5122 (2004).
2. I. Bjedov *et al.*, *Science* **300**, 1404 (2003).
3. V. M. D'Costa, K. M. McGrann, D. W. Hughes, G. D. Wright, *Science* **311**, 374 (2006).
4. M. O. A. Sommer, G. Dantas, G. M. Church, *Science* **325**, 1128 (2009).
5. S. Wright, *J. Am. Stat. Assoc.* **26**, 201 (1931).
6. R. M. May, A. R. McLean, *Theoretical Ecology: Principles and Applications* (Oxford Univ. Press, Oxford, 2007).
7. R. Hermsen, T. Hwa, *Phys. Rev. Lett.* **105**, 248104 (2010).

8. K. Müller, C. Faeh, F. Diederich, *Science* **317**, 1881 (2007).
9. K. Drlica, M. Malik, *Curr. Top. Med. Chem.* **3**, 249 (2003).
10. P. K. Lindgren, A. Karlsson, D. Hughes, *Antimicrob. Agents Chemother.* **47**, 3222 (2003).
11. E. Lautenbach *et al.*, *Arch. Intern. Med.* **162**, 2469 (2002).
12. S. M. Rosenberg, *Nat. Rev. Genet.* **2**, 504 (2001).
13. C. Miller *et al.*, *Science* **305**, 1629 (2004); 10.1126/science.1101630.
14. R. T. Cirz *et al.*, *PLoS Biol.* **3**, e176 (2005).
15. See supporting material on Science Online.
16. S. Park *et al.*, *Science* **301**, 188 (2003).
17. J. E. Keymer, P. Galajda, G. Lambert, D. Liao, R. H. Austin, *Proc. Natl. Acad. Sci. U.S.A.* **105**, 20269 (2008).
18. W. Klaus, A. Ross, B. Gsell, H. Senn, *J. Biomol. NMR* **16**, 357 (2000).
19. M. J. Fath, R. Kolter, *Microbiol. Rev.* **57**, 995 (1993).
20. M. N. Alekshun, S. B. Levy, *Trends Microbiol.* **7**, 410 (1999).
21. H. H. Lee, M. N. Molla, C. R. Cantor, J. J. Collins, *Nature* **467**, 82 (2010).
22. J. E. Barrick *et al.*, *Nature* **461**, 1243 (2009).
23. D. M. Weinreich, N. F. Delaney, M. A. Depristo, D. L. Hartl, *Science* **312**, 111 (2006).
24. G. Lambert *et al.*, *Nat. Rev. Cancer* **11**, 375 (2011).

Acknowledgments: Supported by NSF grant NSF0750323 and National Cancer Institute grant U54CA143803.

The content is solely the responsibility of the authors and does not necessarily represent the official views of the National Cancer Institute or the National Institutes of Health. We thank T. Cox, T. Hwa, N. Goldenfeld, J. Pedersen, S. J. Rahi, S. Rosenberg, and S. Vyawahare for useful discussions, and the referees for useful comments. The reference sequence for the *E. coli* strain K-12 was obtained from GenBank (accession no. NC000913.2). The sequence of the *E. coli* mutant strain was uploaded on the National Center for Biotechnology Information Sequence Read Archive (accession no. SRP007391.10).

Supporting Online Material

www.sciencemag.org/cgi/content/full/333/6050/1764/DC1
Materials and Methods
Figs. S1 to S3
References (25–29)
Movie S1

23 May 2011; accepted 29 July 2011
10.1126/science.1208747

Promoting the Middle East Peace Process by Changing Beliefs About Group Malleability

Eran Halperin,¹ Alexandra G. Russell,² Kali H. Trzesniewski,³ James J. Gross,² Carol S. Dweck^{2*}

Four studies showed that beliefs about whether groups have a malleable versus fixed nature affected intergroup attitudes and willingness to compromise for peace. Using a nationwide sample ($N = 500$) of Israeli Jews, the first study showed that a belief that groups were malleable predicted positive attitudes toward Palestinians, which in turn predicted willingness to compromise. In the remaining three studies, experimentally inducing malleable versus fixed beliefs about groups among Israeli Jews ($N = 76$), Palestinian citizens of Israel ($N = 59$), and Palestinians in the West Bank ($N = 53$)—without mentioning the adversary—led to more positive attitudes toward the outgroup and, in turn, increased willingness to compromise for peace.

Ending long-standing conflicts represents an urgent global challenge. One major barrier to successful conflict resolution is

each group's intensely negative attitudes toward the other group in the conflict (1). Because direct attempts to alter attitudes toward an adversary

can backfire by bringing about defensive reactions (2), we tested the value of a more indirect route: focusing on beliefs about whether groups in general can change.

This focus was suggested by prior research showing that those who believe that people are malleable (versus fixed) are less likely to attribute wrongdoing to a person's fixed qualities, less likely to recommend punishment for a wrongdoer, and more likely to recommend negotiation (3, 4). More specifically, past research has demonstrated that when faced with negative behavior, people who believe that human qualities are malleable are more likely to understand

¹Lauder School of Government, Diplomacy and Strategy, Interdisciplinary Center Herzliya, Herzliya 46150, Israel. ²Department of Psychology, Stanford University, Stanford, CA 94305, USA. ³Human and Community Development, University of California, Davis, CA 95616, USA.

*To whom correspondence should be addressed. E-mail: dweck@stanford.edu